journal

Microstructural Evolution and Formation Mechanism of the Interface Between Titanium and Zirconia Annealed at 1550°C

Kun-Lin Lin and Chien-Cheng Lin*,†

Department of Materials Science and Engineering, National Chiao Tung University, Hsinchu 30050, Taiwan

The diffusional reaction between titanium and zirconia was carried out isothermally at 1550°C in argon. The distinct reaction layers in the reaction-affected zone between Ti and ZrO_2 were investigated using analytical scanning electron microscopy, analytical transmission electron microscopy, and electron probe microanalyses. In the metal side, there existed five reaction layers in a sequence of α-Ti(O), $Ti_2ZrO + \alpha$-Ti(O, Zr), $Ti_2ZrO + \alpha$-Ti(O, Zr) $+ \beta'$-Ti (O, Zr), α-Ti (O, Zr) $+ \beta'$-Ti (O, Zr), and β'-Ti (Zr, O) after cooling. In the zirconia side, two reaction layers were found: near the original interface, β'-Ti coexisted with fine spherical c-ZrO_{2-x} and Chinese-script-like c-ZrO_{2-x}, which dissolved a significant amount of Y_2O_3 in solid solution; further away from the original interface, the coarsened intergranular α-Zr was excluded from metastable ZrO_{2-x}, resulting in the lenticular t-ZrO_{2-x} and ordered c-ZrO_{2-x}. An attempt was made to determine and propose the microstructural evolution and formation mechanism of the reaction layers between titanium and zirconia isothermally annealed at 1550°C.

I. Introduction

EXTENSIVE studies have been carried out on the interface reaction between titanium and zirconia in the last few decades.[1–3] Weber *et al.*[1] indicated that zirconia was blackened by a limited solid solution of titanium in zirconia, when the titanium melt reacted with the ZrO_2 crucible. In discussing the effect of the Ti additive on the microstructure of zirconia at 2000°C/3 h, Ruh *et al.*[2] found that the liquid titanium diffused into zirconia to form various reaction layers. Zhu *et al.*[3] investigated the wettability and the interaction between pure liquid titanium and yttria-stabilized zirconia by the sessile drop method in an Ar atmosphere at 1700°C. They found that there existed two distinct chemical reaction layers in the interface. Recently, Lin and his coworkers[4–6] conducted an intense investigation on the diffusional reaction between titanium and zirconia. Using transmission electron microscopy/energy dispersive spectroscopy (TEM/EDS) analyses, Lin and Lin[4] indicated that an ordered titanium suboxide (Ti_3O) and the orthorhombic lamellae Ti_2ZrO were formed in the solid solution of α-Ti(O) during cooling from 1700°C. In addition to the lamellar Ti_2ZrO and α-Ti(O), Lin and Lin[5] observed the orthorhombic β'-Ti(Zr, O) and a spherical-ordered Ti_2ZrO phase in the metal side after annealing at 1550°C. By focusing upon the zirconia side far away from the original interface of Ti and ZrO_2, Lin and Lin[6] also observed twinned t'-ZrO_{2-x}, lenticular t-ZrO_{2-x}, ordered c-ZrO_{2-x}, and the intergranular α-Zr after the Ti/ZrO_2 diffusion couple was annealed at 1550°C using analytical TEM.

In order to shed light on the microstructural evolution of the various distinct reaction layers between titanium and zirconia, the Ti/ZrO_2 diffusion couple was isothermally annealed in argon at 1550°C for various periods in the present study, and the microstructures were characterized using analytical scanning electron microscopy (SEM), analytical transmission electron microscopy (TEM), and an electron probe microanalyzer (EPMA). Finally, the formation mechanisms, as well as microstructural evolution, of the reaction layers between titanium and zirconia were proposed.

II. Experimental Procedures

Bulk ZrO_2 specimens used in this study were prepared from the powder of 3 mol% Y_2O_3 partially stabilized zirconia (with a nominal composition of >94 wt% $ZrO_2 + HfO_2$ (HfO_2 accounts for approximately 2%–3% of this total), 5.4 wt% Y_2O_3, < 0.001 wt% Fe_2O_3, < 0.01 wt% SiO_2, <0.005 wt% Na_2O, <0.005 wt% TiO_2, <0.02 wt% Cl, <0.005 wt% SO_4^{2-} (Toyo Soda Mfg. Co., Tokyo, Japan) by hot pressing (Model HP50-MTG-7010, Thermal Techno. Inc., Santa Rosa, CA). The bulk ZrO_2 and commercially available titanium billets (with a nominal composition of 99.31 wt% Ti, 0.25 wt% O, 0.01 wt% H, 0.03 wt% N, 0.10 wt% C, 0.30 wt% Fe; Kobe Steel, Ltd., Tokyo, Japan) were cut and machined into dimensions of 14 mm × 14 mm × 5 mm. The sandwiched samples, one Ti in between two ZrO_2 specimens, were slightly pressed and annealed at 1550°C for 0.5, 3, and 6 h in an atmosphere of Ar. The hot-pressing procedures of bulk ZrO_2 and the sandwiched samples have been described in detail elsewhere.[5]

The cross-sectional SEM, TEM, and EPMA specimens perpendicular to the interface of titanium and zirconia were cut, ground, and polished by standard procedures. The microstructures at the interface were observed using an analytical SEM (Model JSM 6500F, JEOL Ltd., Tokyo, Japan) and an analytical TEM (Model JEM 2000Fx, JEOL Ltd.). The quantitative composition analyses were carried out based on the principle of the Cliff–Lorimer standardless technique[7] by an EDS (Mode ISIS300, Oxford Instrument Inc., London, U.K.) attached to the TEM. The backscattered electron images (BEI) had been taken on the SEM. The compositions of those phases in the reaction layers at the interface between Ti and ZrO_2 were quantitatively measured by an EPMA (JXA-8800M, JEOL, Tokyo, Japan) with the aid of an atomic number, absorption, and fluorescence corrections (ZAF) program.[8] The measurement conditions for EPMA were as follows: the accelerating voltage was 15 kV, the probe current was 1.5×10^{-8} A, and the beam diameter was 1 μm.

III. Results and Discussion

(1) Formation Mechanism of Various Reaction Layers

Figures 1(a), (b), and (c) display the backscattered electron images of the cross section normal to the interface between Ti and ZrO_2 after reaction at 1550°C for 0.5, 3, and 6 h, respectively. Titanium was on the left-hand side, while zirconia was on the
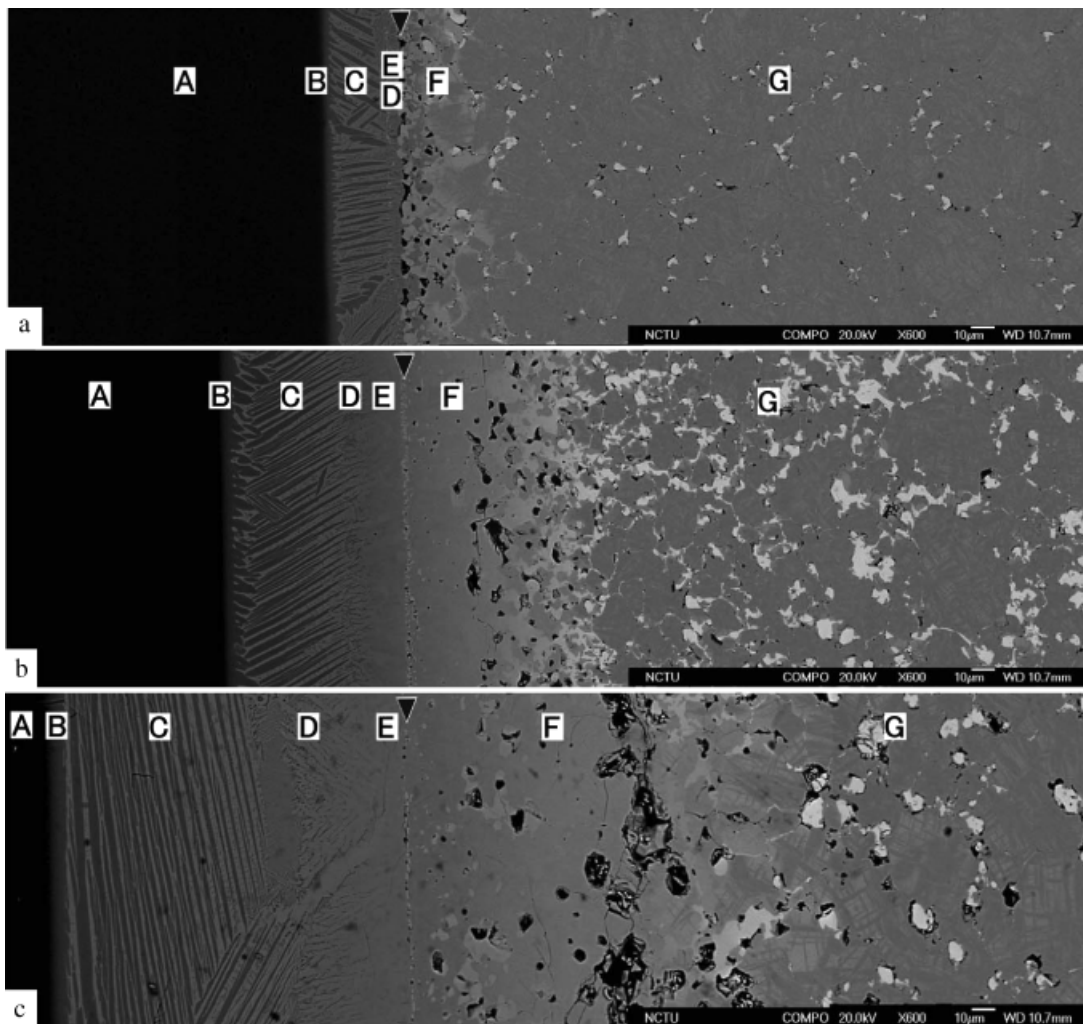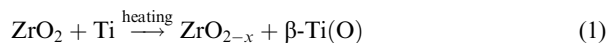

T. Mitchell—contributing editor

Fig. 1. (a), (b), and (c) Scanning electron micrographs (backscattered electron image, BEI) of the cross section between Ti/ZrO$_2$ after reaction at 1550°C/0.5, 3, and 6 h, respectively. The arrows indicate the original interface between Ti/ZrO$_2$.

other side. The arrows in the upper middle of these figures indicated the original interface of Ti and ZrO$_2$. There were five reaction layers, designated as "A," "B," "C," "D," and "E," on the metal side, while only two distinct reaction layers, designated as "F" and "G," were found on the zirconia side. The thickness of the individual reaction layers increased with the annealing time. Moreover, in the reaction layer "G," zirconia grains grew obviously and α-Zr (brighter) was coarsened and became isolated after reaction at 1550°C for 6 h (Fig. 1(c)). The existence of the pores in the ceramic side was attributed to the Kirkendall effect, as zirconium and oxygen diffused to the titanium side much faster than titanium diffused toward the zirconia side.
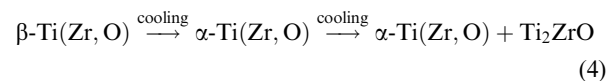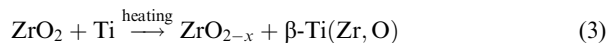
Figure 2(a) displays the backscattered electron image of the cross section normal to the interface between Ti and ZrO$_2$ after reaction at 1550°C/6 h. The distributions of Y, Ti, Zr, and O elements in the interface are demonstrated by X-ray mappings in Figs. 2(b)–(e), respectively. The original interface (the arrows) was deliberately located according to the results of the characteristic $K\alpha$ X-ray map of yttrium (Fig. 2(b)), which was relatively immobile compared with the elements Zr, O, and Ti. Because Ti and Zr are isomorphous elements and the differences in their atomic radii are very small,[9] they are readily substituted for each other. Figures 2(c) and (d) confirm that the interdiffusion of Ti and Zr was intense and the diffusion distance of Ti and Zr was nearly equal. Figure 2(e) shows that oxygen underwent a long-range diffusion into titanium, leading to the formation of the oxygen-containing α-Ti.

Figure 3 displays the backscattered electron image of the reaction layers "A," "B," and "C" between Ti and ZrO$_2$ after

reaction at 1550°C/6 h. The reaction layer "A" was α-Ti, which dissolved a large amount of oxygen and a small amount of zirconium. The quantitative analyses by the EPMA showed that it contained 71.30 at.% Ti, 0.97 at.% Zr, and 27.72 at.% O, Original corresponding to α-Ti(O). α-Ti(O) was formed by the oxidation–reduction reaction of titanium and zirconia, and can be expressed as follows:

$$ZrO_2 + Ti \xrightarrow{\text{heating}} ZrO_{2-x} + \beta\text{-Ti(O)} \tag{1}$$

$$\beta\text{-Ti(O)} \xrightarrow{\text{cooling}} \alpha\text{-Ti(O)} \tag{2}$$

The reaction layer "B" with a continuous lamellar morphology consisted of α-Ti (gray) and needle-like Ti$_2$ZrO (bright). The thin continuous layer, consisting of lamellar α-Ti and Ti$_2$ZrO, was first found in the present study. Unlike these continuous lamellar phases found in the present study, Lin and Lin[5] reported that the Ti$_2$ZrO lamellae were precipitated from plate-like α-Ti (O, Zr) by a eutectoid reaction during cooling. The formation of lamellar α-Ti (O) and Ti$_2$ZrO in the thin continuous layer (the reaction layer "B") can be expressed as follows:

$$ZrO_2 + Ti \xrightarrow{\text{heating}} ZrO_{2-x} + \beta\text{-Ti(Zr, O)} \tag{3}$$

$$\beta\text{-Ti(Zr, O)} \xrightarrow{\text{cooling}} \alpha\text{-Ti(Zr, O)} \xrightarrow{\text{cooling}} \alpha\text{-Ti(Zr, O)} + Ti_2ZrO \tag{4}$$
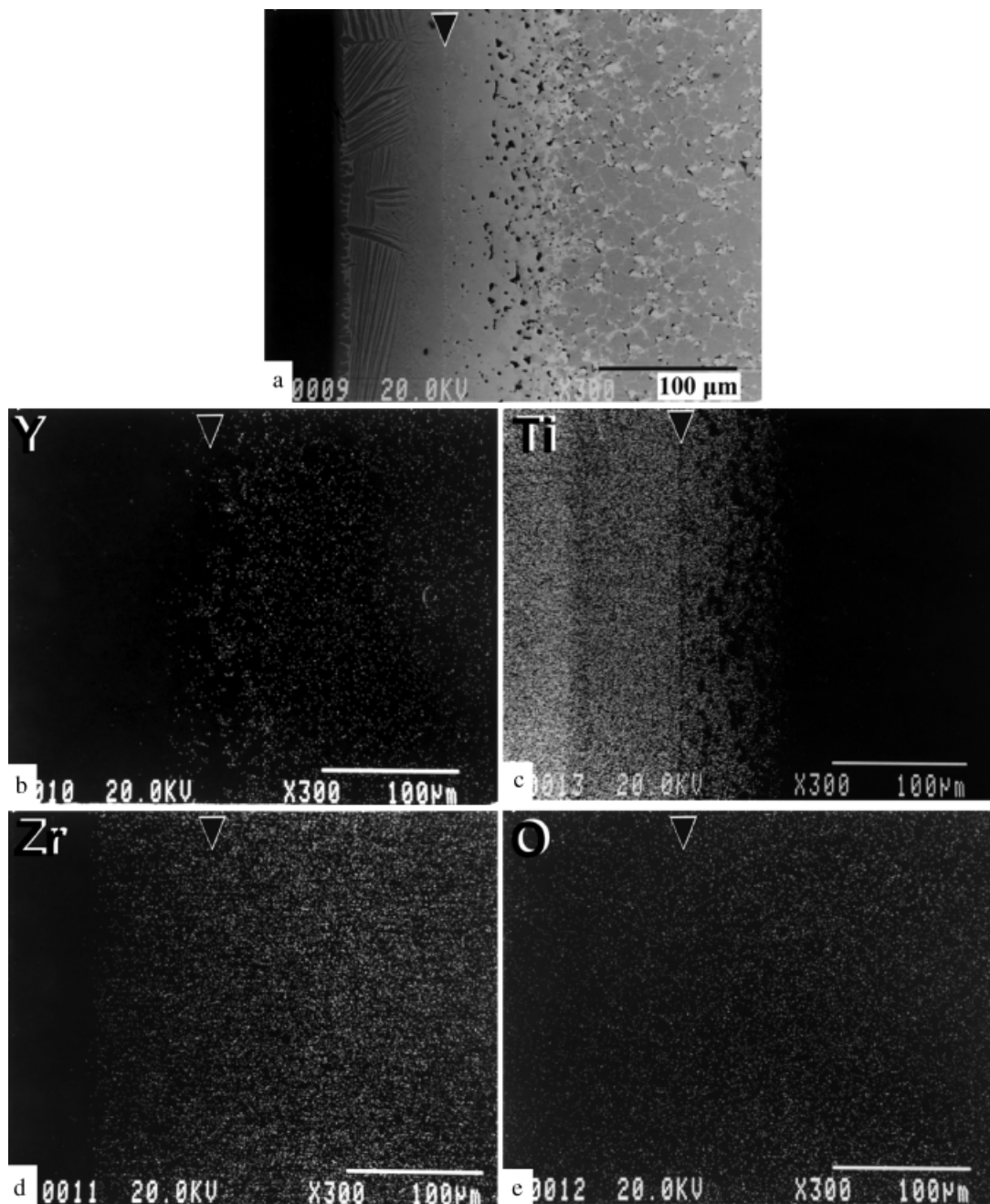
Fig. 2. (a) Scanning electron micrograph (backscattered electron image, BEI) of the cross section between Ti/ZrO$_2$ after reaction at 1550°C/6 h; (b)–(e) X-ray maps of Y, Ti, Zr, and O, respectively.

The reaction layer "C" consisted of β'-Ti (bright) and the lamellae of Ti$_2$ZrO and α-Ti (gray). At high temperatures, the primary α-Ti dissolved a large amount of zirconium and oxygen, forming metastable α-Ti(Zr, O), and thus resulted in the precipitation of the lamellae Ti$_2$ZrO during cooling. Meanwhile, the β-Ti, which dissolved a large amount of Zr and O, transformed into orthorhombic β'-Ti(Zr, O) solid solution during cooling. The coexistence of α-Ti (O), Ti$_2$ZrO, and β'-Ti (O, Zr) can be expressed by the following reactions:

$$ZrO_2 + Ti \xrightarrow{\text{heating}} ZrO_{2-x} + \alpha\text{-Ti(Zr, O)} + \beta\text{-Ti(Zr, O)} \quad (5)$$

$$\alpha\text{-Ti(Zr, O)} + \beta\text{-Ti(Zr, O)}$$
$$\xrightarrow{\text{cooling}} \alpha\text{-Ti(Zr, O)} + Ti_2ZrO + \beta'\text{-Ti(Zr, O)} \quad (6)$$
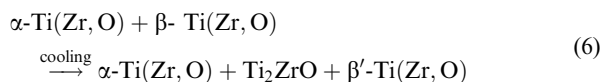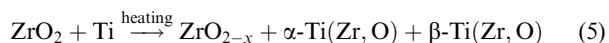
Figure 4 displays the backscattered electron image of the reaction layer "D" in the interface between Ti and ZrO$_2$ after

reaction at 1550°C/6 h. The original interface of titanium and zirconia was beyond the right-hand side of the micrograph. When the concentration of zirconium is like that in the region on the left-hand side of Fig. 4, the reaction layer "D" would consist of the acicular α-Ti (dark) in the β-Ti matrix (gray). The precipitation of the acicular α-Ti(O, Zr) can be expressed as follows:

$$ZrO_2 + Ti \xrightarrow{\text{heating}} ZrO_{2-x} + \beta\text{-Ti(Zr, O)} \quad (3)$$

$$\beta\text{-Ti(Zr, O)} \xrightarrow{\text{cooling}} \alpha\text{-Ti(Zr, O)} + \beta'\text{-Ti(Zr, O)} \quad (7)$$
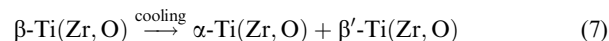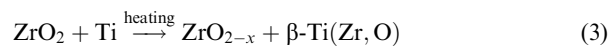
As zirconium was the stabilizer of β-Ti, fewer acicular α-Ti was observed on the right-hand side of Fig. 4, where a higher concentration of Zr existed in titanium. Also shown in Fig. 4, the amount of the acicular α-Ti increased with the distance away from interface. The reaction layer "D," which dissolved a significant amount of zirconium (β stabilizer) and oxygen (α stabilizer), was composed of α+β titanium with Zr and O in solid
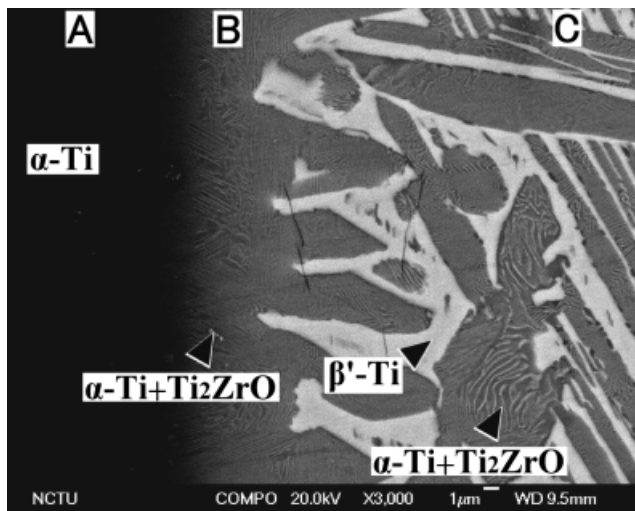
Fig. 3. Scanning electron micrograph (backscattered electron image, BEI) of the reaction layers "A," "B," and "C" in the interface between Ti/ZrO$_2$ after reaction at 1550°C/6 h.

solution. For comparison, it is worth noting that the acicular-like α-Ti was also found in α+β titanium alloys such as Ti–6Al–4V or Ti–8Al–1Mo–1 alloys.[10]

The orientation relationship of the acicular α-Ti and the β'-Ti has been subjected to an intense investigation. Figure 5(a) shows the TEM micrograph (bright-field image, BFI) of the reaction layer "D" viewed in the direction normal to the interface of Ti and ZrO$_2$ after reaction at 1550°C/6 h. The acicular α-Ti and the β'-Ti were identified as hexagonal and orthorhombic crystal structures, respectively, from the superimposed selected area diffraction patterns (SADPs), as shown in Fig. 5(b). The SADPs in Fig. 5(b) were schematically redrawn in Fig. 5(c), with the diffraction spots being indexed. The orientation relations between α-Ti and β'-Ti were thus identified as follows: $[2\bar{1}\bar{1}0]_{\alpha\text{-Ti}}$ // $[001]_{\beta'\text{-Ti}}$ and $(0001)_{\alpha\text{-Ti}}$// $(100)_{\beta'\text{-Ti}}$. Moreover, the lattice constants of the β'-Ti orthorhombic unit cell were calculated as follows: $a_o = 0.58$ nm, $b_o = 0.84$ nm, and $c_o = 0.61$ nm, and those of the α-Ti hexagonal unit cell were $a_h = b_h = 0.30$ nm, and $c_h = 0.46$ nm. Figure 5(d) shows the EDS spectrum of the acicular α-Ti, revealing that it comprised 54.0 at.% Ti, 13.4 at.% Zr, and 32.8 at.% O. Figure 5(e) shows the EDS spectrum of the β'-Ti, consisting of 58.1 at.% Ti, 30.7 at.% Zr, and 11.2 at.% O. As Zr is a stabilizer of β-titanium, it is not surprising that β'-Ti(Zr, O) contains much more Zr than α-Ti(Zr, O) does.

Fig. 5. (a) Transmission electron micrograph (bright-field image, BFI) of the reaction layer "D" after reaction at 1550°C/6 h; (b) and (c) selected area diffraction patterns of the α-Ti and β'-Ti, $Z = [2\bar{1}\bar{1}0]_{\alpha\text{-Ti}}//[0\,0\,1]_{\beta'\text{-Ti}}$ and its schematic diagram (Δ, α-Ti; ○, β'-Ti), respectively; (d) and (e) energy-dispersive spectra of α-Ti and β'-Ti.

Figure 6(a) also shows the TEM micrograph (BFI) of the reaction layer "D" viewed in the direction normal to the interface of Ti and ZrO$_2$ after reaction at 1550°C/6 h. Another orientation relationship of the acicular α-Ti and the β'-Ti was identified by the superimposed SADPs (Fig. 6(b)). The SADPs were redrawn and indexed in Fig. 6(c). The orientation relations were recognized as follows: $[2\bar{1}\bar{1}0]_{\alpha\text{-Ti}}$// $[021]_{\beta'\text{-Ti}}$ and $(0001)_{\alpha\text{-Ti}}$ // $(1\bar{1}2)_{\beta'\text{-Ti}}$. Figure 6(d) displays the image, taken from the high-resolution transmission electron microscopy (HRTEM), of the acicular α-Ti and the β'-Ti. The d-spacing of the plane $(01\bar{1}0)$ for α-Ti was equal to 0.50 nm, while that of the $(3\bar{1}2)$ plane for β'-Ti was equal to 0.28 nm. The high-resolution image, as shown in Fig. 6(e), of the marked area in Fig. 6(d) was simulated by a computer program (Digital Micrograph 3.3, Gatan Inc., Pleasanton, CA). It indicated that the ledge mechanism (labeled as "L") was probably the favorable precipitation mechanism of α-Ti from the matrix of β'-Ti. The ledge mechanism was frequently encountered in the partially coherent interface, consisting of many sets of edge dislocations or misfit dislocations. When the crystal structures of the matrix and the precipitate were different to a signif-
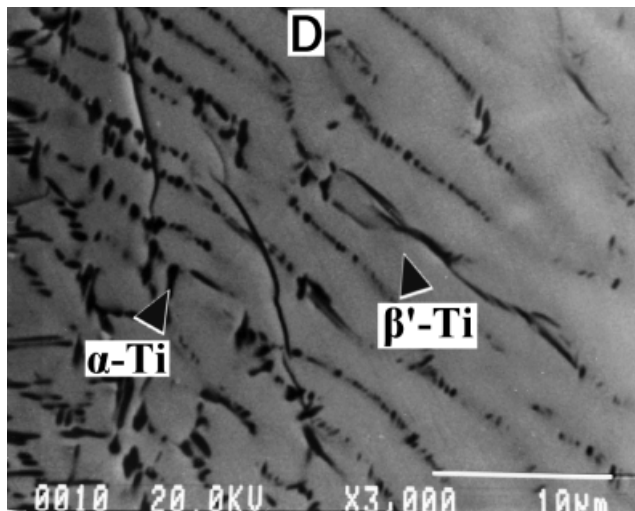

Fig. 4. Scanning electron micrograph (backscattered electron image, BEI) of the reaction layer "D" in the interface between Ti/ZrO$_2$ after reaction at 1550°C/6 h.
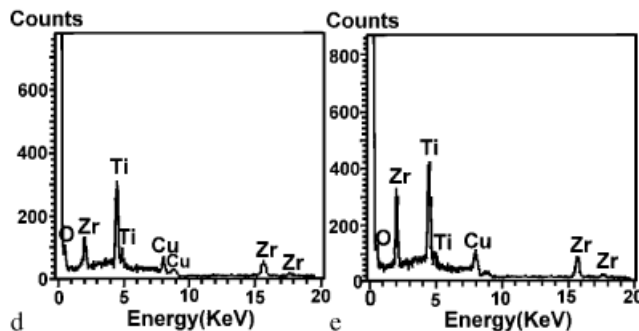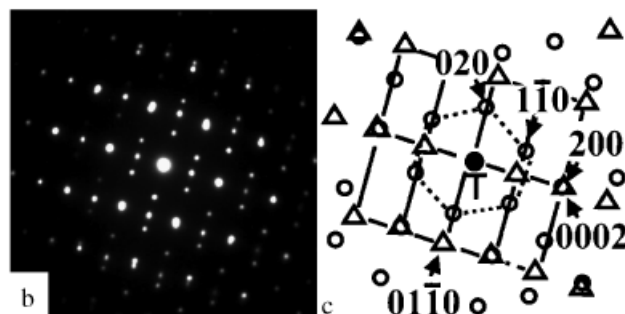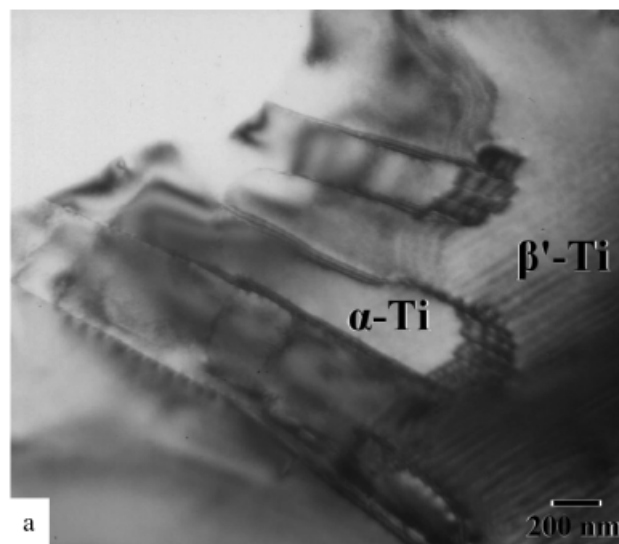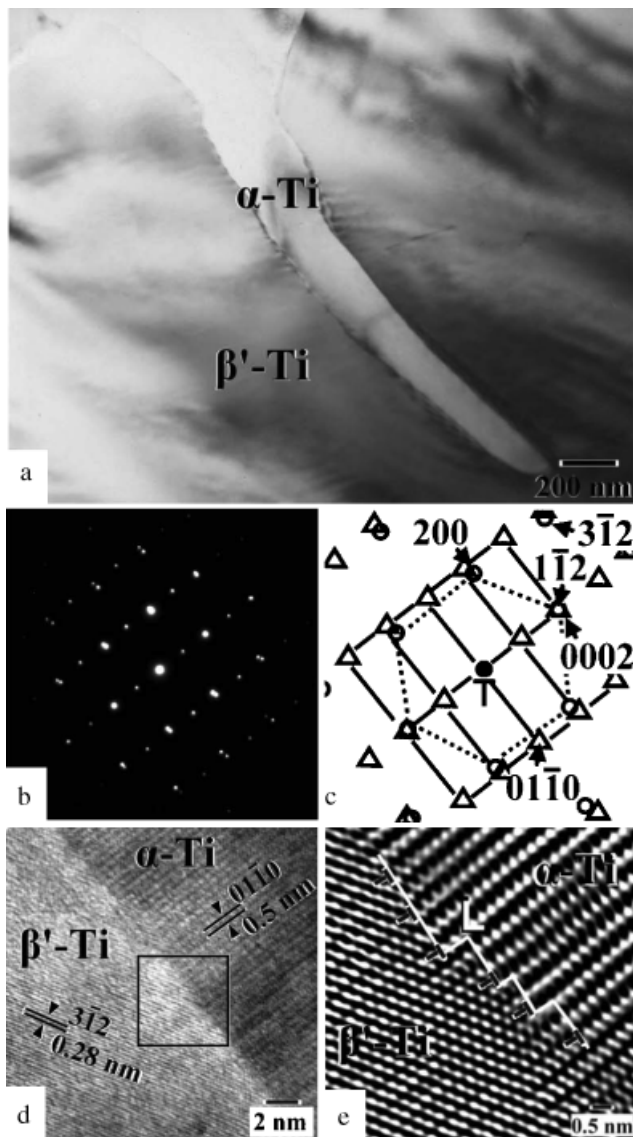
Fig. 6. (a) Transmission electron micrograph (bright-field image, BFI) of the reaction layer "D" after reaction at 1550°C/6 h; (b) and (c) selected area diffraction patterns of the α-Ti and β'-Ti, $Z = [2\,\bar{1}\,\bar{1}\,0]_{\alpha\text{-Ti}}//[0\,2\,1]_{\beta'\text{-Ti}}$ and its schematic diagram (Δ, α-Ti; ○, β'-Ti), respectively; (d) images taken from the high-resolution transmission electron microscopy of acicular α-Ti and β'-Ti; (e) the computer simulation of the marked area in Fig. 6(d).

icant degree, the interface boundaries had to migrate by the ledge mechanism.[11] The ledge mechanism was reported, for instance, to be the growth mechanism of α and β interface boundaries in a Ti-based alloy.[12] It was likely that the acicular α-Ti was also precipitated from a β'-Ti matrix by means of the ledge mechanism.

Figure 7 shows the backscattered electron image of the reaction layers "E" and "F," together with "D" between Ti and ZrO$_2$ after reaction at 1550°C/6 h. The arrows in the upper middle indicate the original interface of Ti and ZrO$_2$. Abutting the zirconia side, the precipitate-free reaction layer "E" (gray), which dissolved a large amount of zirconium and oxygen, was β'-Ti in the solid solution, consisting of 35.33 at.% Ti, 25.85 at.% Zr, and 38.82 at.% O measured by the EPMA. The formation of β'-Ti in the solid solution, designated as β'-Ti(Zr, O), can be expressed as follows:

$$ZrO_2 + Ti \xrightarrow{\text{heating}} ZrO_{2-x} + \beta\text{-Ti}(Zr, O) \quad (3)$$

$$\beta\text{-Ti}(Zr, O) \xrightarrow{\text{cooling}} \beta'\text{-Ti}(Zr, O) \quad (8)$$

Fig. 7. Scanning electron micrograph (backscattered electron image, BEI) of the reaction layers "D," "E," and "F" in the interface between Ti/ZrO$_2$ after reaction at 1550°C/6 h.

In contrast, β'-Ti (gray) and c-ZrO$_{2-x}$ (bright, either rounded or Chinese script like) coexisted in the reaction layer "F." On performing EPMA analyses, it was found that this β'-Ti contained 46.72 at.% Ti, 27.00 at.% Zr and 26.28 at.% O; meanwhile, the Chinese-script-like c-ZrO$_{2-x}$ contained 2.36 at.% Ti, 20.92 at.% Zr, 66.87 at.% O, and 9.84 at.% Y, displaying a large amount of yttrium, an effective stabilizer of c-ZrO$_{2-x}$. This is the reason why the zirconia was cubic symmetric in crystal structure. A few small rounded c-ZrO$_{2-x}$ grains were scattered near the interface, as c-ZrO$_{2-x}$ grains were extensively dissolved into titanium. On the right-hand side of Fig. 7, a Chinese-script-like c-zirconia phase (resembling the stroke of a calligraphic brush) was surrounded by the β'-Ti. The reason why c-ZrO$_{2-x}$ became Chinese script like was still unclear at present. It was believed that zirconium was excluded from the metastable oxygen-deficient zirconia during cooling. However, no α-Zr was found in the reaction layer "F" like in the reaction layer "G," as zirconium went into the solid solution in β'-Ti (O, Zr). The formation mechanisms in the reaction layer "F" can be expressed as follows:

$$ZrO_2 + Ti \xrightarrow{\text{heating}} ZrO_{2-x} + \beta\text{-Ti}(Zr, O) \quad (3)$$

$$ZrO_{2-x} \xrightarrow{\text{cooling}} \alpha\text{-Zr} + c\text{-ZrO}_{2-y(y<x)} \quad (9)$$

$$\alpha\text{-Zr} + c\text{-ZrO}_{2-y(y<x)} + \beta\text{-Ti}(Zr, O)$$
$$\xrightarrow{\text{cooling}} c\text{-ZrO}_{2-y(y<x)} + \beta'\text{-Ti}(Zr, O) \quad (10)$$
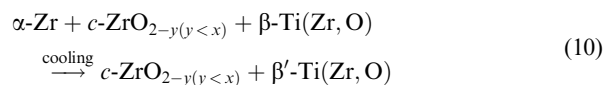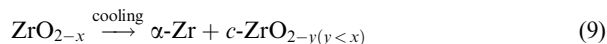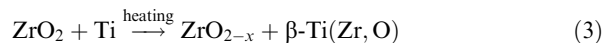
Figure 8 displays the backscattered electron image and various characteristic X-ray maps of the reaction layer "F" after reaction at 1550°C/6 h. The X-ray mapping of Y in Fig. 8(b) indicates that yttrium was hardly dissolved in titanium and then remained in both small spherical and Chinese-script-like zirconia. This is consistent with the results reported by Zhu *et al.*,[3] who found that the yttrium element congregated and remained at the interface to form a high Y$_2$O$_3$ content of ZrO$_2$ when ZrO$_2$ reacted with molten titanium. The distributions of Ti, Zr, and O elements in the reaction layer "F" (Figs. 8 (c)–(e)) indicated that a significant amount of titanium diffused into the ceramic side and reacted with zirconia to form β'-Ti(Zr, O).

Figure 9(a) displays the backscattered electron image of the reaction layer "G" in the zirconia side far away from the interface after reaction at 1550°C/6 h. The distributions of Y, Ti, Zr, and O elements in the interface are demonstrated by individual characteristic X-ray mappings in Figs. 9(b)–(e), respectively. It
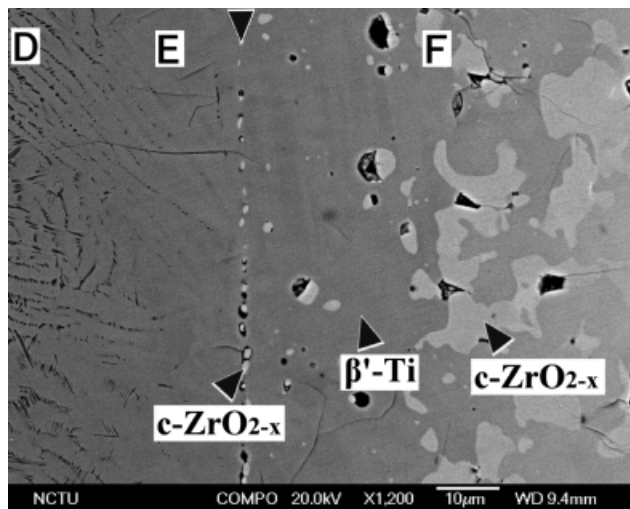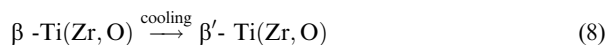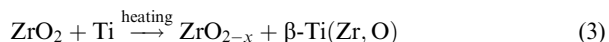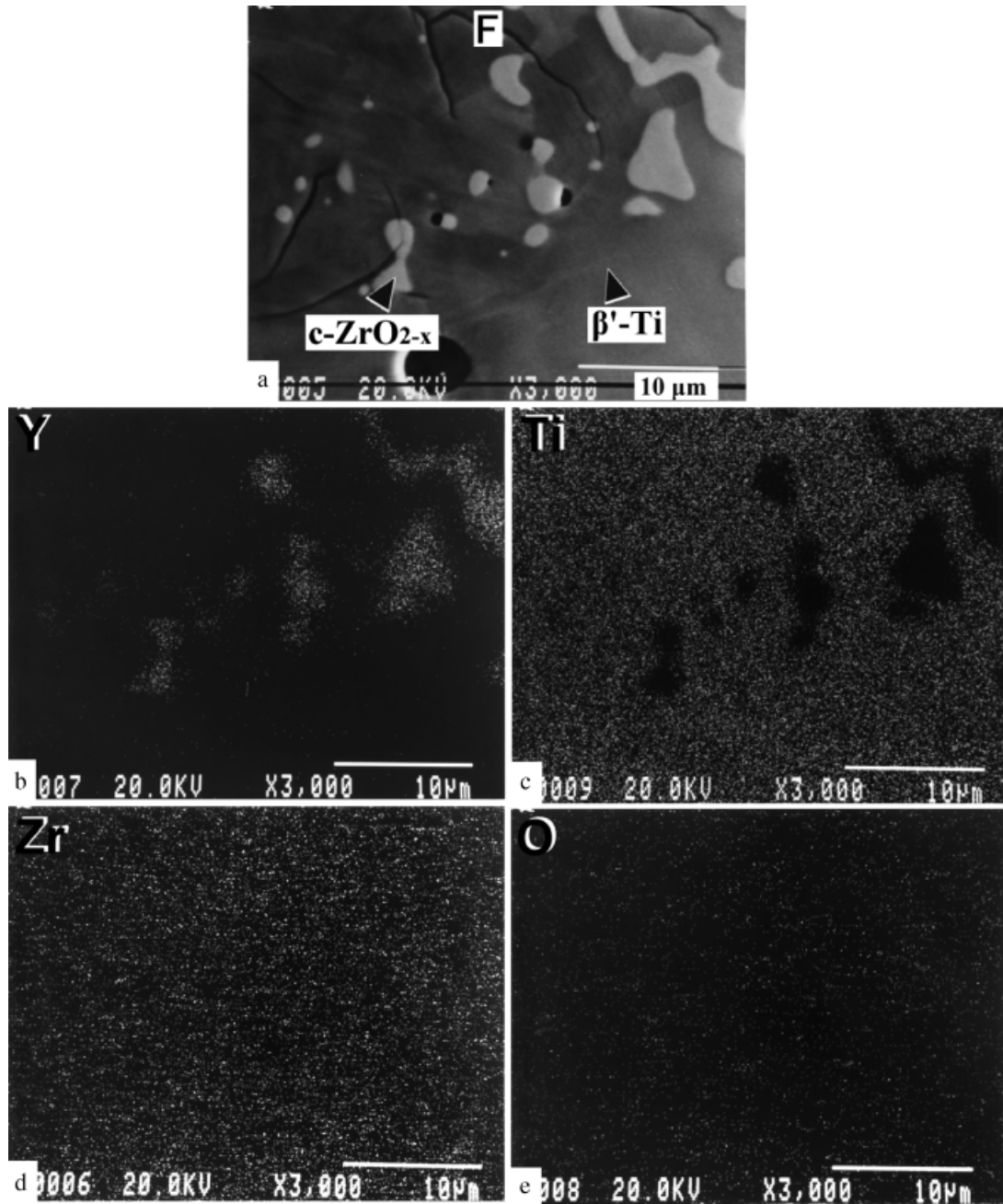
Fig. 8. (a) Scanning electron micrograph (backscattered electron image, BEI) of the reaction layer "F" in the interface between Ti/ZrO$_2$ after reaction at 1550°C/6 h; (b)–(e) X-ray maps of Y, Ti, Zr, and O, respectively.

indicates that a significant amount of oxygen was dissolved in α-Zr (bright), with both yttrium and titanium being hardly dissolved in α-Zr. From the EMPA analyses, the α-Zr in the reaction layer "G" contained 1.05 at.% Ti, 57.5 4 at.% Zr, 40.73 at.% O, and 0.68 at.% Y, corresponding with α-Zr (O). Because the content of Zr in *c*- or *t*-ZrO$_{2-x}$ declined as the temperature decreased, as shown in the Zr–O phase diagram,[13] the α-Zr was segregated on grain boundaries during cooling by the exsolution of zirconium from ZrO$_{2-x}$, causing an increase in the O/Zr ratio of oxygen-deficient zirconia.

The *c*-ZrO$_{2-x}$ and the lenticular *t*-ZrO$_{2-x}$ were observed in the gray region (Fig. 9(a)). It was believed that the specimen was cooled down from the two-phase (*c*+*t*) region in the ZrO$_2$–Y$_2$O$_3$ phase diagram. The fact that the lenticular *t*-ZrO$_2$ with three variants was transformed in the *c*-ZrO$_{2-x}$ had been reported by several previous studies.[6,14–17] Lin and Lin[6] further found that the lenticular *t*-ZrO$_{2-x}$ was formed in an ordered *c*-ZrO$_{2-x}$. It was worth noting that zirconia grains with a concentrated

yttrium (Fig. 9(b)) had a cubic symmetry in crystal structure. The formation mechanisms in the reaction layer "G" can be expressed as follows:

$$ZrO_2 + Ti \overset{heating}{\longrightarrow} ZrO_{2-x} + \beta\text{-}Ti(O) \tag{1}$$

$$ZrO_{2-x} \overset{cooling}{\longrightarrow} \alpha\text{-}Zr(O) + c\text{-}ZrO_{2-y(y<x)} + t\text{-}ZrO_{2-y(y<x)} \tag{11}$$
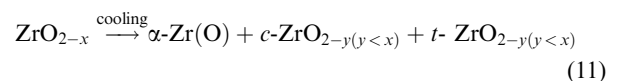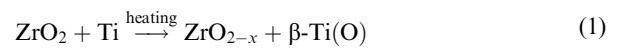
Based upon the foregoing results and discussion, the individual phases and formation mechanisms of the distinct reaction layers in the reaction-affected zone between titanium and zirconia have been summarized in Table I.

(2) Proposed Model of Microstructural Evolution

Even though extensive studies were carried out on the interface reaction between titanium and zirconia, the microstructure
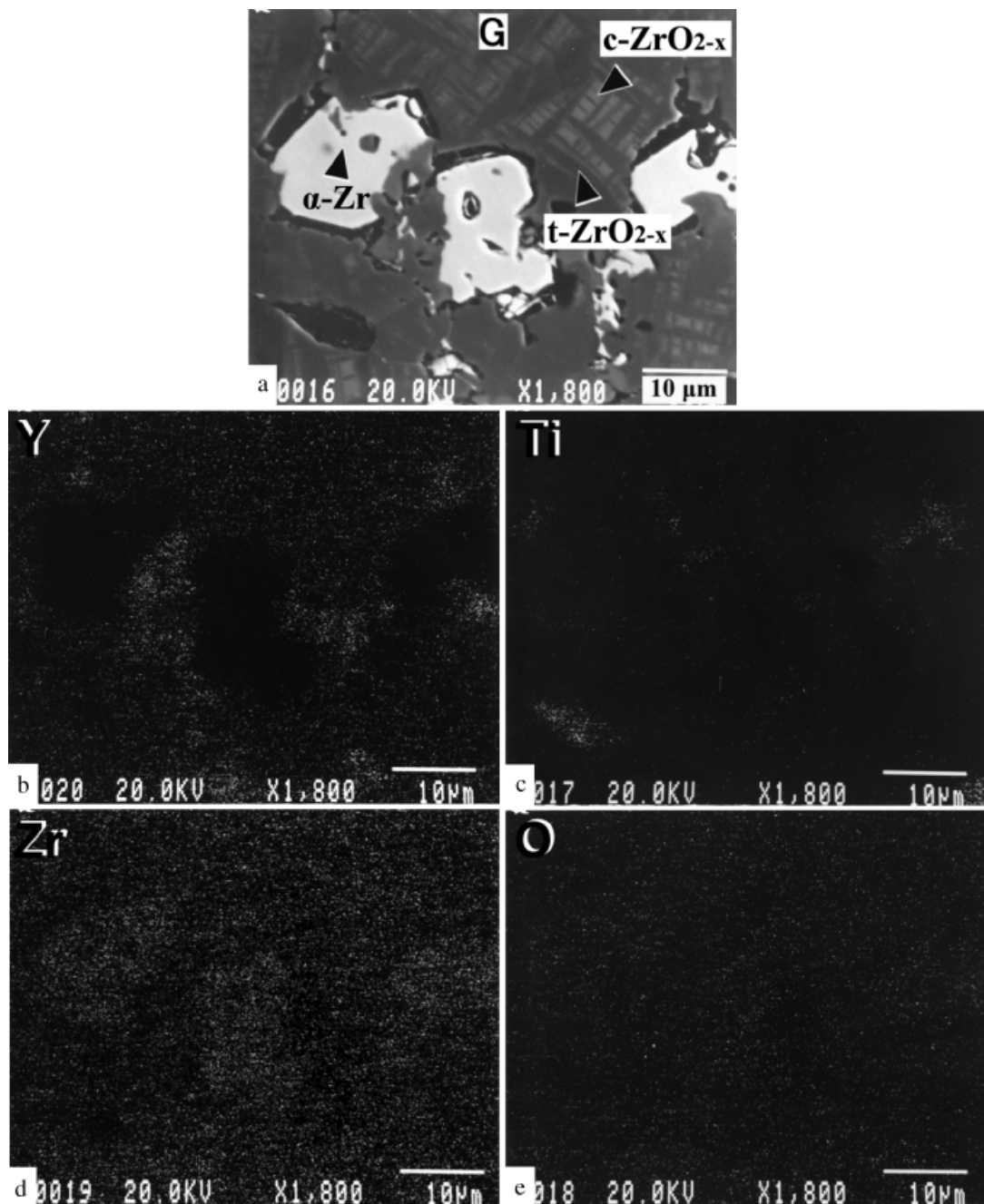
Fig. 9. (a) Scanning electron micrograph (backscattered electron image, BEI) of the reaction layer "G" in the zirconia side away from the interface after reaction at 1550°C/6 h; (b)–(e) X-ray maps of Y, Ti, Zr, and O, respectively.

evolution has not yet been elucidated to date. The information with regard to the relationships between the ternary constitution and the microstructures produced by isothermal diffusion among three elements is very sparse.[18] In the present study, an attempt has been made to infer the microstructure resulting from isothermal diffusion among titanium and zirconia with the aid of the Ti–Zr–O ternary phase diagram. However, only the isothermal Ti–Zr–O ternary phase diagram at 1450°C (not 1550°C) has been found in the literature.[19] Assuming that the compositions of the solid phases are approximated as constant between 1450° and 1550°C, the interpretation of the microstructure at the interface between Ti and ZrO_2 in terms of the Ti–Zr–O phase diagram can be reasonably determined. The Ti–Zr–O phase diagram and the diffusion couple are somewhat different chemically. The ZrO_2 contains 3 mol% Y_2O_3, so it is out of the Ti–Zr–O ternary system. However, this probably does not have much effect on the results, and the effect may be negligible in this study.

Figure 10 shows the microstructural evolution at the interface between a titanium and zirconia diffusion couple after annealing at 1550°C based upon the observation and analyses mentioned above. Figure 10(a) illustrates the titanium and zirconia diffusion couple prior to the anneal heat treatment, indicating the original interface and finely distributed ZrO_2 grains. When titanium was held in contact with zirconia at high temperatures, various diffusion layers developed.

By cross examining the experimental results and the ternary phase diagram, it was proposed that all gross compositions, in various vertical slices along the longitudinal direction perpendicular to the interface, lay upon the line a–b–c–d–e, or the so-called diffusion path, in the Ti–Zr–O ternary system at 1450°C.[19] As shown in Fig. 10(b), the diffusion path crosses the fields of β-Ti, α-Ti+β-Ti, β-Ti, β-Ti+t-ZrO_2, α-Zr+β-Ti+ t-ZrO_2, and α-Zr+t-ZrO_2.

It is well known that the divariant or three-phase regions in the ternary phase diagram are simply in correspondence to the

Table I. Microstructural Features and Formation Mechanisms of Various Phases at the Interface of Ti and ZrO₂ at 1550°C

Ti/ZrO₂ diffusion couple	Reaction layer	Phases	Formation mechanisms
Metal side	"A"	α-Ti(O)	Eqs. (1) and (2)
	"B"	α-Ti(Zr, O) Ti₂ZrO	Eqs. (3) and (4)
	"C"	α-Ti(Zr, O) Ti₂ZrO β'-Ti(Zr, O)	Eqs. (5) and (6)
	"D"	α-Ti(Zr, O) β'-Ti	Eqs. (3) and (7)
	"E"	β'-Ti(Zr, O)	Eqs. (3) and (8)
Zirconia side	"F"	β'-Ti(Zr, O) c-ZrO₂₋ₓ	Eqs. (3), (9), and (10)
	"G"	α-Zr(O) t-ZrO₂₋ₓ c-ZrO₂₋ₓ	Eqs. (1) and (11)

interfaces between layers in the diffusion couple, which is isothermally annealed at high temperatures. Conversely, ternary isothermal diffusion can result in the formation of both one-phase and two-phase layers in the diffusion couple, but not three-phase layers.[18] As a result, in the Ti–ZrO₂ diffusion couple, the layers of β-Ti, α-Ti+β-Ti, β-Ti, β-Ti+*t*-ZrO₂, and α-Zr+*t*-ZrO₂ would have been observed in sequence from Ti to ZrO₂, but not the layers of α-Zr+β-Ti+*t*-ZrO₂. The region of α-Zr+β-Ti+*t*-ZrO₂ in the Ti–Zr–O ternary phase diagram was represented in the diffusion couple by the interface between the layers of β-Ti+*c*-ZrO₂ and α-Zr+*c*-ZrO₂ as shown in Fig. 10(c). Furthermore, as illustrated in Fig. 10(b), the β-Ti layer, corresponding to the layer "A," varied in composition from Ti to β_a. The α in the α-Ti+β-Ti layer should vary from α_a to α_b and the β from β_a to β_b, while the β-Ti, corresponding to layers "D" and "E," varied from β_b to β_c.

In the case of a Ti–ZrO₂ diffusion couple where the reaction was predominant in the initial stage and the diffusion velocities of the three components were markedly different, the diffusion path deviated from the direct path between the compositions of the end points, i.e., Ti and ZrO₂ in the present study. It was believed that the oxidation–reduction reaction in the initial stage shifted the end point in the ceramic side to the two-phase region of α-Zr+*t*-ZrO₂, presumably to point *e*. Besides, it was unlikely that the diffusion path passed the region of α-Ti+β-Ti+*t*-ZrO₂ as it was impossible for such an interface to exist in between the layers of α-Ti+β-Ti and β-Ti+*t*-ZrO₂. It was also noted that the layer of α-Zr+β-Ti was not observed in the present study. As a consequence, the ternary diffusion path *a–b–c–d–e* provided the best approximation that could be made at present.

In reality, the high chemical affinity of titanium to oxygen led to the formation of oxygen-deficient zirconia (ZrO₂₋ₓ), indicating that the oxidation–reduction reaction predominated in the initial stage before the diffusion prevailed. A significant increase in oxygen vacancies, as a consequence of the oxidation–reduction reaction between titanium and zirconia, triggered the stabilization effect of zirconia. The zirconia in the Ti–Zr–O ternary phase diagram, shown in Fig. 10(b), was in the cubic phase instead of tetragonal phase when the Ti/ZrO₂ diffusion couple was isothermally annealed at 1550°C.[6]

The various layers formed during the cooling stage are displayed in Fig. 10(d). The β-Ti layer abutting the reaction-unaffected Ti, with a small amount of Zr in solid solution, was transformed to α-Ti (designated as layer "A") on cooling, and the continuous lamellar Ti₂ZrO+α-Ti (designated as layer "B") is attributed to the precipitation of Ti₂ZrO in the metastably transformed α-Ti matrix. Ti₂ZrO was precipitated from α-Ti in the α-Ti+β-Ti layer during cooling, leading to the existence of

Fig. 10. Schematic diagrams showing the microstructural evolution of the Ti/ZrO₂ diffusion couple annealed at 1550°C. (a) As hot pressed; (b) the diffusion path drawn in the Ti–Zr–O ternary phase diagram at 1450°C[19]; (c) the structure of the Ti/ZrO₂ diffusion couple on annealing at 1550°C, and (d) the structure on cooling.

the lamellar (Ti₂ZrO+α-Ti)+β'-Ti region (designated as layer "C"). In the layer "D," the β-Ti was transformed to β'-Ti where the acicular α-Ti was precipitated; meanwhile, a continuous β'-Ti(Zr, O) with a large amount of Zr in solid solution was found near the interface (designated as layer "E"). On the zirconia side, the dissolution of zirconia in titanium led to the formation of β-Ti(Zr, O) and the dissolution of titanium in zirconia suppressed the grain growth of zirconia near the interface. During cooling, β'-Ti(Zr, O) and cubic ZrO₂₋ₓ, with high yttrium, were formed in the reaction layer "F." Because of very low solubility in titanium, almost all of the yttrium remained in zirconia, resulting in the stabilization of *c*-ZrO₂₋ₓ during cooling down to room temperature. Away from the original metal–ceramic interface, ZrO₂ was dramatically reduced to ZrO₂₋ₓ by titanium, accompanied by a significant grain growth of ZrO₂₋ₓ on heating. The intergranular α-Zr was excluded from the metastable oxygen-deficient zirconia, while the lenticular *t*-ZrO₂ and ordered *c*-ZrO₂₋ₓ were formed from the *c*-ZrO₂₋ₓ matrix during cooling (the reaction layer "G").

IV. Conclusions

1. The diffusional reaction between titanium and zirconia was carried out at 1550°C in argon. On the metal side, there existed five reaction layers in a sequence of α-Ti(O), Ti₂ZrO+α-Ti(O, Zr), Ti₂ZrO+α-Ti(O, Zr)+β'-Ti (O, Zr), α-Ti (O, Zr)+β'-Ti (O, Zr), and β'-Ti (Zr, O) after cooling.

2. On the zirconia side, two reaction layers were found: near the original interface, β'-Ti coexisted with fine spherical c-ZrO$_{2-x}$ and Chinese-script-like c-ZrO$_{2-x}$; further away from the original interface, coarsened intergranular α-Zr, lenticular t-ZrO$_{2-x}$, and ordered c-ZrO$_{2-x}$ were found.

3. The acicular α-Ti and the β'-Ti showed two different orientation relations. One of the orientation relations was determined to be $[2\bar{1}\bar{1}0]_{\alpha\text{-Ti}}$ // $[001]_{\beta'\text{-Ti}}$ and $(0001)_{\alpha-\text{Ti}}$ // $(100)_{\beta'\text{-Ti}}$ and the other was $[2\bar{1}\bar{1}0]_{\alpha\text{-Ti}}$ //$[021]_{\beta'\text{-Ti}}$ and $(0001)_{\alpha-\text{Ti}}$// $(1\bar{1}2)_{\beta'\text{-Ti}}$.

4. Based upon the experimental results in this study, the diffusion path, connecting phases formed by the reaction between Ti and ZrO$_2$, was drawn on the Ti–Zr–O ternary phase diagram.

5. The information with regard to the relationships between the Ti–Zr–O ternary phase diagram and the microstructures produced by isothermal diffusion between Ti and ZrO$_2$ at 1550°C has been provided.

References

[1] B. C. Weber, H. J. Garrett, F. A. Mauer, and M. A. Schwartz, "Observations on the Stabilization of Zirconia," *J. Am. Ceram. Soc*, **39** [6] 197–207 (1956).

[2] R. Ruh, N. M. Tallan, and H. A. Lipsitt, "Effect of Metal Additions on the Microstructure of Zirconia," *J. Am. Ceram. Soc*, **47** [12] 632–5 (1964).

[3] J. Zhu, A. Kamiya, T. Yamada, W. Shi, K. Naganuma, and K. Mukai, "Surface Tension, Wettability and Reactivity of Molten Titanium in Ti/Yttria-Stabilized Zirconia System," *Mater. Sci. Eng. A*, **A327**, 117–27 (2002).

[4] K. F. Lin and C. C. Lin, "Transmission Electron Microscope Investigation of the Interface Between Titanium and Zirconia," *J. Am. Ceram. Soc*, **82** [11] 3179–85 (1999).

[5] K. L. Lin and C. C. Lin, "Ti$_2$ZrO Phases Formed in the Titanium and Zirconia Interface after Reaction at 1550°C," *J. Am. Ceram. Soc*, **88** [5] 1268–72 (2005).

[6] K. L. Lin and C. C. Lin, "Zirconia-Related Phases in the Zirconia/Titanium Diffusion Couple after Annealing at 1100° to 1550°C," *J. Am. Ceram. Soc*, **88** [10] 2928–34, (2005).

[7] G. Cliff and G. W. Lorimer, "The Quantitative Analysis of Thin Specimens," *J. Microsc.*, **130** [3] 203–7 (1975).

[8] J. I. Goldstein, *Scanning Electron Microscopy and X-ray Microanalysis*, 2nd edition, Plenum Press, New York, 1992.

[9] J. L. Murray and H. A. Wriedt, "The Titanium–Zirconium System"; pp. 340–5 in *Phase Diagrams of Binary Titanium Alloys*, Edited by J. L. Murray. ASM International, Metals Park, OH, 1987.

[10] G. Lutjering and J. C. Williams, *Titanium*; Chapter 5, p. 177. Springer-Verlag, Berlin, Germany, 2003.

[11] D. A. Porter and K. E. Easterling, *Phase Transformations in Metals and Alloys*. Chapman & Hall, New York, 1992.

[12] T. Furuhara, H. J. Lee, E. S. K. Menon, and H. I. Aaronson, "Interphase Boundary Structures Associated with Diffusional Phase Transformations in Ti-Base Alloys," *Metall. Trans. A*, **21A**, 1627–43 (1990).

[13] H. Baker, *ASM Handbook, Vol. 3, Alloy Phase Diagrams*, p. 2326. ASM International, Metals Park, OH, 1992.

[14] A. H. Heuer and M. Rühle, "Phase Transformations in ZrO$_2$-Containing Ceramic: I, The Instability of c-ZrO$_2$ and the Resulting Diffusion-Controlled Reactions"; pp. 1–13 in *Advances in Ceramics, Vol. 12, Science and Technology of Zirconia II*, Edited by N. Claussen, M. Rühle, and A. H. Heuer. American Ceramic Society, Columbus, OH, 1984.

[15] V. Lanteri, A. H. Heuer, and T. E. Mitchell, "Tetragonal Phase in the System ZrO$_2$–Y$_2$O$_2$"; pp. 118–30 in *Advances in Ceramics, Vol. 12, Science and Technology of Zirconia II*, Edited by N. Claussen, M. Rühle, and A. H. Heuer. American Ceramic Society, Columbus, OH, 1984.

[16] R. Chaim, M. Rühle, and A. H. Heuer, "Microstructural Evolution in a ZrO$_2$–12 Wt% Y$_2$O$_3$ Ceramic," *J. Am. Ceram. Soc*, **68** [8] 27–31 (1985).

[17] A. H. Heuer, V. Lanteri, and A. Dominguez-Rodriguez, "High-Temperature Precipitation Hardening of Y$_2$O$_3$ Partially-Stabilized ZrO$_2$ (Y-PSZ) Single Crystals," *Acta Metall*, **37** [2] 559–67 (1989).

[18] F. N. Rhines, *Phase Diagrams in Metallurgy: Their Development and Application*, pp. 156–7. McGraw-Hill Book Company, New York, OH, 1965.

[19] H. M. Ondik, and H. F. McMurdie (eds.), *Phase Diagrams for Zirconium+Zirconia Systems*, p. 12. The American Ceramic Society, OH, 1998.　　□